Hindawi Publishing Corporation
International Journal of Photoenergy
Volume 2012, Article ID 857567, 5 pages
doi:10.1155/2012/857567

Research Article

Layer-by-Layer CdS-Modified TiO_2 Film Electrodes for Enhancing the Absorption and Energy Conversion Efficiency of Solar Cells

Ming Li,[1,2] Yong Liu,[1] Hai Wang,[1,2] Wenxia Zhao,[2] Hong Huang,[2] Chaolun Liang,[3] Youjun Deng,[1] and Hui Shen[1]

[1] *School of Physics and Engineering and State Key Laboratory of Optoelectronic Materials and Technologies and Institute for Solar Energy Systems, Sun Yat-sen University, Guangzhou 510275, China*
[2] *School of Chemical and Biologic Engineering, Guilin University of Technology, Guilin 541004, China*
[3] *Instrumental Analysis and Research Center, Sun Yat-sen University, Guangzhou 510275, China*

Correspondence should be addressed to Yong Liu, liuyong7@mail.sysu.edu.cn

Received 14 November 2011; Accepted 31 January 2012

Academic Editor: Peter Rupnowski

A layer-by-layer assemble method was used to fabricate CdS quantum dots (QDs) sensitized electrodes. Scanning electron microscopy (SEM), energy-dispersive X-ray spectroscopy (EDS), and transmission electron microscopy (TEM) have been utilized to characterize the samples. The absorption spectra and photovoltaic measurement confirmed that much more effective deposition of QDs in TiO_2 matrix and much better power conversion performance were achieved for these multilayer electrodes compared with the ones fabricated by traditional single-layer assembly method.

1. Introduction

In recent years, dye-sensitized solar cells (DSSCs) have attracted a lot of scientific and technological interests owing to their high energy conversion efficiency, low production cost, and a facile fabrication process [1–3]. Besides conventional ruthenium dyes, inorganic short-band-gap semiconductor quantum dots, such as CdS, CdSe, CdTe, PbS and others, have been researched as the good candidate sensitizers in the so-called quantum-dot-sensitized solar cell (QD-SSC) [4–7]. The advantage of inorganic QDs over conventional ruthenium dyes is that QDs can generate multiple electron-hole pairs per proton and improve the efficiency of the solar cells [8]. In addition, QDs' optic and electronic properties can be adjusted to match the solar spectrum much better by changing their shape and size [9–11]. However, the difficulty of penetrating QDs into the mesoporous TiO_2 matrix hindered QD-SSCs from achieving higher energy conversion efficiency. The QDs assembly difficulty can mainly be attributed to the two following reasons: (1) QDs are generally not bound effectively to the TiO_2 crystalline surface to form a firmly anchoring QDs monolayer on TiO_2 nanoparticles [12]. (2) It is relatively difficult for nanoscale QDs to penetrate deep into the TiO_2 mesoporous films and deposit in the underlayer of TiO_2 film. To solve the first problem, the various bifunctional surface modifiers are adopted as linker molecules to anchor the QDs on TiO_2 surface, which indeed enhance assembly of QDs [13–15]. But little attention focused on the second problem. It is still unachievable to obtain an entire coverage of QDs on the surface of TiO_2 crystal throughout the mesoporous films.

In this work, we used multilayered quantum dots assembly method to fabricate CdS QDs sensitized solar cells. The increased coverage ratio, incorporation amount of QDs, and effective deposition of QDs in underlayer of TiO_2 mesoporous films were expected for these multilayer CdS quantum-dots-sensitized solar cells.

2. Experimental Details

8 g TiO_2 powder (P25, Degussa) was thoroughly mixed with 100 mL distilled water by vigorous stirring and ultrasonic. The slurry was then sprayed on transparent conductive oxide (TCO) glass (14 Ω/squ, Nippon Sheet Glass) and the films were dried at 120°C for 10 min. For CdS quantum dot

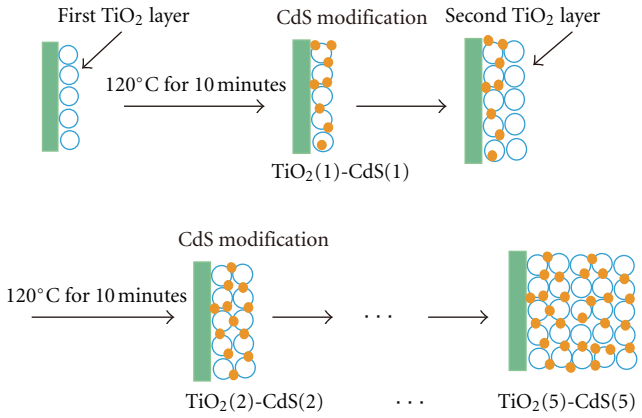

Figure 1: The preparation process of multilayer CdS-sensitized TiO_2 electrodes.

deposition, the TiO_2 films were immersed in 20 mL solution containing 0.002 mmol $Cd(NO_3)_2$, 1 mmol thiourea, and 0.02 mol $NH_3 \cdot H_2O$ and heated up to 60°C for two hours. The as-prepared samples were cleaned sequentially with distilled water. The spraying-drying-depositing procedure was termed as one SDD cycle. One to five cycles were applied to fabricate the $TiO_2(n)$-CdS(n) electrodes (n = 1–5). The process used for the preparation of the $TiO_2(n)$-CdS(n) electrodes was displayed in Figure 1. For comparison, one-step (abbr. OS) preparation of TiO_2 film (TiO_2(OS)) with almost same thickness as $TiO_2(5)$ was also fabricated. CdS deposition process was similar to the procedure ascribed above except the longer CdS bath time of 10 h. TiO_2(OS)-CdS and multilayer $TiO_2(n)$-CdS(n) (n = 1–5) electrodes were all annealed at 400°C for 30 min in nitrogen.

A surlyn spacer (30 μm thick, DuPont) was sandwiched between the CdS quantum-dot-sensitized electrode and the Pt-coated counterelectrode. The space between the electrodes was filled with the polysulphide electrolyte which consisted of Na_2S (0.5 M), S (0.125 M), and KCl (0.2 M), using water/methanol (7 : 3 by volume) solution as co-solvent. A 0.25 cm^2 active area was defined by a hole punched through the surlyn frame and was additionally masked from illumination by black electrical tape to the same size.

The morphology and chemical composition of photoanode were examined by field-emission scanning electron microscopy (FESEM, JSM-6330F) equipped with an energy-dispersive X-ray spectrometer (EDS) analyzer. The detailed microscopic characterization of CdS QDs was analyzed using transmission electron microscope (TEM, JEM-2010HR). Absorption spectra of samples were recorded using a spectrophotometer (Hitachi U-4100). The photocurrent-voltage (I-V) curve of each cell was measured by Keithley 2400 source meter under an illumination of a solar simulator (Newport Oriel 91192) at 100 mW cm^{-2}. Electron impedance spectroscopy (EIS) measurements were carried out by applying a 10 mV AC signal over the frequency range of 10^{-2}–10^5 Hz under 100 mW cm^{-2} illumination at open circuit voltage by using an electrochemical workstation (CHI760C).

3. Results and Discussion

Figures 2(a) and 2(b) are the SEM images of TiO_2 film before and after CdS quantum dots deposition, respectively. The bare nanocrystalline TiO_2 film was exhibited in Figure 2(a). After CdS modification, there was a coating assembled on the surface of TiO_2 nanoparticles (Figure 2(b)). The EDS analysis (Figure 2(c)) confirmed that this coating consist of CdS. Figure 2(d) shows the TEM image of the CdS nanocrystal. The distance of 0.337 and 0.245 nm between the adjacent lattice fringes can be assigned to the interplanar distance of hexagon CdS (002) and (102) face, respectively. The diameter of QDs was about in the range of 5~10 nm.

Figure 3 shows the comparison of the absorption spectrum of multilayer electrodes. The absorbance intensities of electrodes increased with SDD cycles. The absorption peaks of CdS-modified electrodes with different cycles were almost at same position of 450 nm, which was consistent to the value reported in the literature [16]. For $TiO_2(5)$-CdS(5), the absorption edge was approximately 510 nm, which was obtained from the intersection of the sharply decreasing region of a spectrum with its baseline. Corresponding to this absorption edge, the band gap was calculated to be 2.43 eV. That was higher than 2.25 eV, the value reported for CdS in bulk [16]. It indicated that the size of the CdS particles deposited on the TiO_2 films were still within the scale of quantum dots. The size of CdS particles was possible to be estimated from the excitonic peaks of the absorption spectra based on the empirical equations proposed by Yu et al. [17]. Then the mean diameter of CdS particles deposited on the TiO_2 films was calculated to be ca. 8.23 nm. The size of CdS calculated based on empirical equations was consistent with that observed in TEM image. For comparison, the UV-Vis absorption spectra of TiO_2(OS)-CdS was also showed in Figure 3. The absorbance of TiO_2(OS)-CdS was lower than that of $TiO_2(5)$-CdS(5) although their film thickness were almost the same, which displayed the superiority of multilayered electrodes in depositing quantum dots. The absorption edge of TiO_2(OS)-CdS was also at ca. 510 nm, indicating that the size of CdS particles on TiO_2(OS) was the same as that on multilayered electrodes.

The effect of SDD cycles on the device performance has also been studied. The photocurrent-voltage (I-V) curves of the QD-SSCs using $TiO_2(n)$-CdS(n) (n = 1–5) and TiO_2(OS)-CdS as photoelectrodes were showed in Figure 4. It was considered that the absorption spectrum of photoelectrodes played an important role in determining the energy conversion efficiency of DSSCs. Inferred from Figures 3 and 4, the I-V properties of $TiO_2(n)$-CdS(n) QD-SSCs (n = 1–5) were consistent to the absorbance of $TiO_2(n)$-CdS(n) electrodes (n = 1–5). Table 1 summarizes the open circuit potential (V_{OC}), short circuit current density (J_{SC}), fill factor (FF), and overall energy conversion efficiency (η) of these cells. The V_{OC}, J_{SC} and η increased with cycles and the QD-SSC using $TiO_2(5)$-CdS(5) photoelectrode exhibited the best performance due to the most incorporated amount of CdS on electrode. The V_{OC}, J_{SC}, and η of TiO_2(OS)-CdS QD-SSC were only 0.31 V, 0.91 mA cm^{-2}, and 0.11%, respectively, which were much lower than those of $TiO_2(5)$-CdS(5)

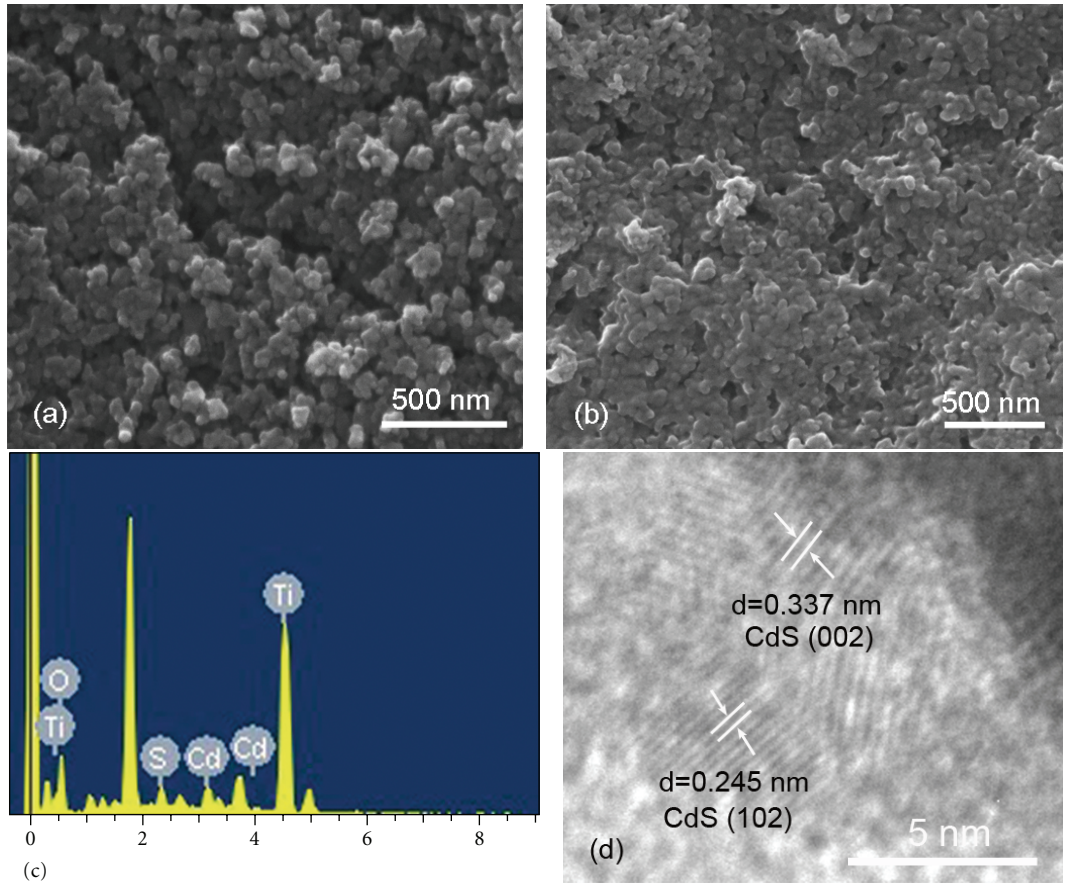

Figure 2: SEM images of TiO_2 nanocrystalline film (a) before and (b) after CdS quantum dots deposition. (c) EDS spectra of CdS-modified TiO_2. (d) TEM image of CdS quantum dots.

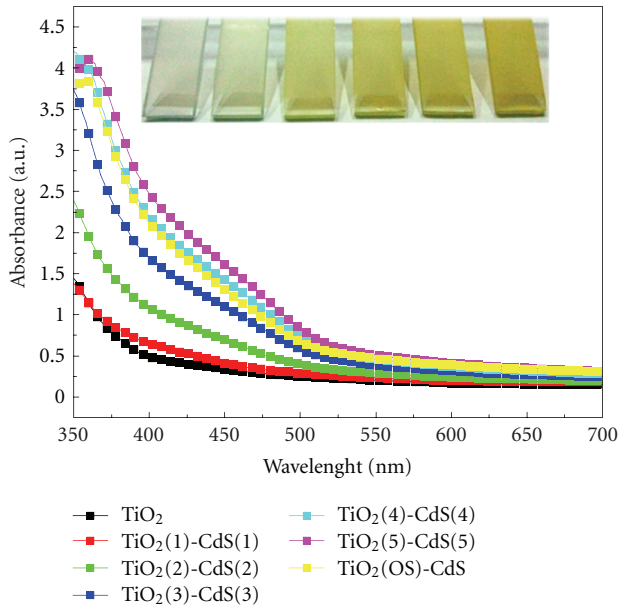

Figure 3: UV-vis absorption spectra of bare TiO_2 nanocrystalline film, $TiO_2(n)$-CdS(n) (n = 1–5) and TiO_2(OS)-CdS electrodes. Photographs of bare TiO_2 and $TiO_2(n)$-CdS(n) (n = 1–5), electrodes were presented in turn as inset.

QD-SSC (0.44 V, 7.12 mA cm^{-2}, and 1.06%), although its absorbance was little lower than that of $TiO_2(5)$-CdS(5). It may be due to the difficulty for CdS QDs diffusing and depositing in the underlayer of TiO_2 mesoporous film, which resulted in overloading of CdS QDs in the surface of TiO_2 film. Overloading of QDs was reported to be disadvantageous to the cell performance because mesopores were blocked by extra loading of CdS QDs and the electrolyte diffusion was also hindered [18]. So the advantage of multilayer TiO_2 films in cell performance over the traditional TiO_2 films was evident. The sealed multilayer CdS QDSSCs displayed good stability still retaining over 90% of their initial efficiency after 720 h of storage in ambient conditions. Here we used only CdS QDs as multilayer sensitizer in this work. It is very promising to deposit different kinds of QDs, such as CdSe, CdTe, and PbSe and the others in multilayers of electrodes. The extending of absorption range, the increase of absorbance, and improvements in the cell efficiency could be possible for solar cell fabricated by multilayer TiO_2 film sensitized by multiple QDs with different absorption spectra range.

Electron impedance spectroscopy of multilayer QD-SSCs, shown in Figure 5, were measured to investigate the kinetics of charge transfer and recombination. An equivalent

Table 1: A summary of photovoltaic and photoelectron transport properties of CdS QD-SSCs under AM1.5 condition.

Sample	V_{OC} (V)	J_{SC} (mA cm^{-2})	FF (%)	η (%)	R_k (Ω)	k_{eff} (s^{-1})	τ_{eff} (s)	$D_{eff} \times 10^8$ (cm^2/s)	Film thickness (μm)
TiO_2(1)-CdS(1)	0.16	0.91	35.2	0.05	308.75	8.291	0.121	3.770	1.2
TiO_2(2)-CdS(2)	0.33	1.71	30.5	0.17	254.86	6.876	0.145	5.331	2.8
TiO_2(3)-CdS(3)	0.42	3.58	29.4	0.44	228.15	3.167	0.316	8.251	3.9
TiO_2(4)-CdS(4)	0.42	5.40	29.9	0.66	197.18	4.663	0.214	24.193	4.9
TiO_2(5)-CdS(5)	0.44	7.12	33.7	1.06	157.33	5.638	0.177	43.264	5.6
TiO_2(OS)-CdS	0.31	0.91	37.9	0.11	312.71	6.876	0.145	38.763	5.8

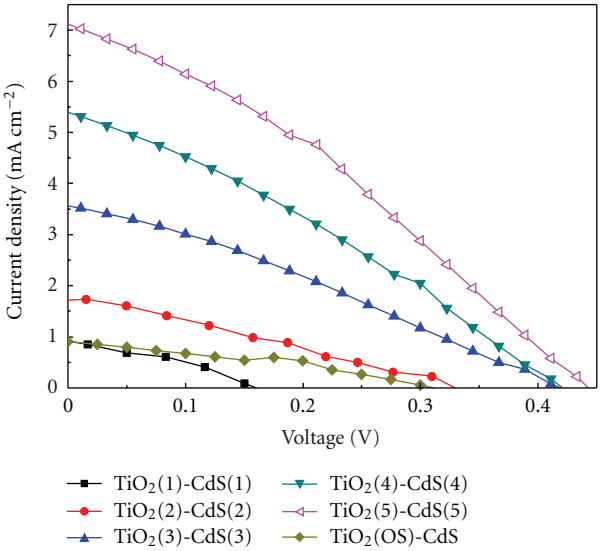

Figure 4: Photocurrent-voltage curves of CdS QD-SSCs measured under AM1.5 condition. The active surface area was 0.25 cm^2.

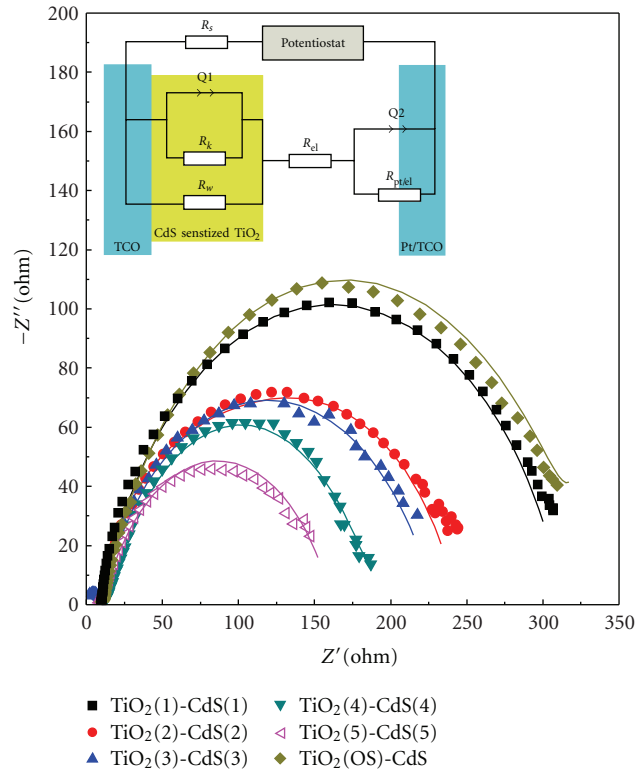

Figure 5: Experimental (dots) and fitted (solid curve) Nyquist plots of CdS QD-SSCs under AM1.5 condition. The equivalent circuit used to fit the experimental data was shown as inset.

circuit used to fit the experimental data was shown as inset in Figure 5. By modeling and fitting the Nyquist plots, the electron transport parameters such as charge transfer resistance related to recombination of electrons at the TiO_2/electrolyte interface (R_k), the first-order reaction rate constant for loss of electrons (k_{eff}), electron life time (τ_{eff}) and effective diffusion coefficient (D_{eff}) were extracted and also presented in Table 1. It was clear that R_k decreased with the SDD cycles, for which there are two possible reasons: (1) an increase in film thickness and (2) an increase in the electron density owing to the increasing current density. k_{eff} decreased with cycles varying from 1 to 3. Thus, the recombination rate decreased with cycles when cycle was below 3. This showed the reason the value of J_{SC} and η increases greatly when cycles were within 3. But k_{eff} increased when cycle was more than 3. The increasing recombination rate means that electrons were lost rapidly by recombination. Inferred from Table 1, although FF decreased with cycle changing from 1 to 3 and then increased when cycle was above 3, the growth rate of η for cells with cycle above 3 decreased comparing with that for ones with cycle below 3 under considering the rate of increase for film thickness. It was deduced that the increase of electron recombination rate may contribute to the decreasing growth rate of η above 3 SDD cycles. D_{eff} increased with the increasing film thickness, which was consistent with the result reported by Adachi et al. [19]. As for TiO_2(OS)-CdS, the R_k value was similar with that of TiO_2(1)-CdS(1), which should due to similar current density of these two cells.

4. Conclusion

We have demonstrated a layer-by-layer assembling method to improve the coverage of QDs on the surface of TiO_2 crystal throughout the mesoporous films effectively and its application in QD sensitized solar cells. The multilayer electrodes showed much more effective deposition of QDs in TiO_2 matrix and better power conversion performance, compared with the ones fabricated by traditional method.

The open circuit voltage, short circuit current, and overall power conversion efficiencies of multilayer CdS QD-SSCs increased with the layers and reached maximum value, 0.44 V, 7.12 mA cm^{-2}, and 1.06%, respectively, for 5 layers.

Acknowledgments

The authors gratefully acknowledge financial support from National Basic Research Program of China (973 Program) (no. 2012CB933704), the Fundamental Research Funds for the Central Universities (no. 10lgpy17), the Research Fund of State Key Laboratory of Optoelectronic Materials and Technologies, China (no. 2010-RC-3-3), and the Production and Research Project of Guangdong Province and Ministry of Education, China (no. 2010B090400020).

References

[1] B. O'Regan and M. Grätzel, "A low-cost, high-efficiency solar cell based on dye-sensitized colloidal TiO_2 films," *Nature*, vol. 353, no. 6346, pp. 737–740, 1991.

[2] M. Grätzel, "Photoelectrochemical cells," *Nature*, vol. 414, no. 6861, pp. 338–344, 2001.

[3] M. Grätzel, "Solar energy conversion by dye-sensitized photovoltaic cells," *Inorganic Chemistry*, vol. 44, no. 20, pp. 6841–6851, 2005.

[4] Y. Zhang, T. Xie, T. Jiang et al., "Surface photovoltage characterization of a ZnO nanowire array/CdS quantum dot heterogeneous film and its application for photovoltaic devices," *Nanotechnology*, vol. 20, no. 15, Article ID 155707, 2009.

[5] K. S. Leschkies, R. Divakar, J. Basu et al., "Photosensitization of ZnO nanowires with CdSe quantum dots for photovoltaic devices," *Nano Letters*, vol. 7, no. 6, pp. 1793–1798, 2007.

[6] C. Ratanatawanate, C. Xiong, and K. J. Balkus, "Fabrication of PbS quantum dot doped TiO_2 nanotubes," *ACS Nano*, vol. 2, no. 8, pp. 1682–1688, 2008.

[7] X. Cao, P. Chen, and Y. Guo, "Decoration of textured ZnO nanowires array with CdTe quantum dots: enhanced light-trapping effect and photogenerated charge separation," *Journal of Physical Chemistry C*, vol. 112, no. 51, pp. 20560–20566, 2008.

[8] A. J. Nozik, "Exciton multiplication and relaxation dynamics in quantum dots: applications to ultrahigh-efficiency solar photon conversion," *Inorganic Chemistry*, vol. 44, no. 20, pp. 6893–6899, 2005.

[9] L. Bakueva, I. Gorelikov, S. Musikhin, X. S. Zhao, E. H. Sargent, and E. Kumacheva, "PbS quantum dots with stable efficient luminescence in the near-IR spectral range," *Advanced Materials*, vol. 16, no. 11, pp. 926–929, 2004.

[10] C. Ghosh, S. Pal, P. Sarkar, and T. Frauenheim, "Size and composition dependent electronic and optical properties of $Ga_xAl_{1-x}As$ and $Al_xGa_{1-x}As$ alloyed nanocrystals," *Applied Physics Letters*, vol. 94, no. 12, Article ID 123105, 3 pages, 2009.

[11] D. More, C. Rajesh, A. D. Lad, G. R. Kumar, and S. Mahamuni, "Two photon absorption in Mn^{2+}-doped ZnSe quantum dots," *Optics Communications*, vol. 283, no. 10, pp. 2150–2154, 2010.

[12] G. Y. Lan, Z. Yang, Y. W. Lin, Z. H. G. Lin, H. Y. Liao, and H. T. Chang, "A simple strategy for improving the energy conversion of multilayered CdTe quantum dot-sensitized solar cells," *Journal of Materials Chemistry*, vol. 19, no. 16, pp. 2349–2355, 2009.

[13] Y. J. Shen and Y. L. Lee, "Assembly of CdS quantum dots onto mesoscopic TiO_2 films for quantum dot-sensitized solar cell applications," *Nanotechnology*, vol. 19, no. 4, Article ID 045602, 2008.

[14] I. Mora-Seró, S. Giménez, T. Moehl et al., "Factors determining the photovoltaic performance of a CdSe quantum dot sensitized solar cell: the role of the linker molecule and of the counter electrode," *Nanotechnology*, vol. 19, no. 42, Article ID 424007, 2008.

[15] N. Guijarro, T. Lana-Villarreal, I. Mora-Seró, J. Bisquert, and R. Gómez, "CdSe quantum dot-sensitized TiO_2 electrodes: effect of quantum dot coverage and mode of attachment," *Journal of Physical Chemistry C*, vol. 113, no. 10, pp. 4208–4214, 2009.

[16] Y. L. Lee and Y. S. Lo, "Highly efficient quantum-dot-sensitized solar cell based on co-sensitization of CdS/CdSe," *Advanced Functional Materials*, vol. 19, no. 4, pp. 604–609, 2009.

[17] W. W. Yu, L. Qu, W. Guo, and X. Peng, "Experimental determination of the extinction coefficient of CdTe, CdSe, and CdS nanocrystals," *Chemistry of Materials*, vol. 15, no. 14, pp. 2854–2860, 2003.

[18] P. Sudhagar, J. H. Jung, S. Park et al., "The performance of coupled (CdS:CdSe) quantum dot-sensitized TiO_2 nanofibrous solar cells," *Electrochemistry Communications*, vol. 11, no. 11, pp. 2220–2224, 2009.

[19] M. Adachi, M. Sakamoto, J. Jiu, Y. Ogata, and S. Isoda, "Determination of parameters of electron transport in dye-sensitized solar cells using electrochemical impedance spectroscopy," *Journal of Physical Chemistry B*, vol. 110, no. 28, pp. 13872–13880, 2006.